

Surface Plasmon Resonance-Based Fiber-Optic Hydrogen Gas Sensor Utilizing Indium–Tin Oxide (ITO) Thin Films

Satyendra K. Mishra · Banshi D. Gupta

Received: 4 November 2011 / Accepted: 5 March 2012 / Published online: 1 April 2012
© Springer Science+Business Media, LLC 2012

Abstract We report experimental study on an indium–tin oxide (ITO)-coated surface plasmon resonance-based fiber-optic hydrogen gas sensor operating at room temperature. The sensor works on intensity modulation interrogation. Indium–tin oxide ($\text{In}_2\text{O}_3+\text{SnO}_2$) films were grown on unclad core of the fiber by thermal evaporation technique. The surface plasmon resonance (SPR) spectra for 100 % nitrogen gas as well as for a mixture of 4 % hydrogen gas and 96 % nitrogen gas were obtained. In the case of mixture of hydrogen and nitrogen gases, a sharp dip in the SPR spectrum was observed implying that the hydrogen gas changes the dielectric properties of ITO. The performance of the sensor has been studied for different percentages of tin oxide in indium oxide and for different thicknesses of ITO film. Both the parameters have been optimized for the best performance of the sensor.

Keywords Surface plasmon · Optical fiber · Sensor · Indium–tin oxide ($\text{In}_2\text{O}_3:\text{SnO}_2$) · Hydrogen gas · Nitrogen gas

Introduction

For the last few decades, surface plasmon resonance (SPR) technique has been widely used for the detection of several physical, chemical, and biochemical parameters [1, 2]. In this technique, a p-polarized light causes the excitation of charge density oscillation called surface plasmon wave along the metal-dielectric interface by satisfying the resonance condition. The surface plasmon wave is TM polarized

and its electric field decays exponentially in metal as well as in dielectric. The propagation constant of the surface plasmon wave can be obtained by solving the Maxwell's equation for a metal-dielectric interface and is given by

$$K_{sp} = \frac{\omega}{c} \left(\frac{\varepsilon_m \varepsilon_s}{\varepsilon_m + \varepsilon_s} \right)^{\frac{1}{2}} \quad (1)$$

where ε_m and ε_s represent the dielectric constants of the metal and the dielectric medium, respectively; ω represents the frequency of incident light and c is the velocity of the light in vacuum. Equation (1) is valid for the case where two media (metal and dielectric) are semi-infinite. The maximum value of the propagation constant of the light wave at frequency ω propagating through the dielectric medium is given by

$$K_s = \frac{\omega}{c} \sqrt{\varepsilon_s} \quad (2)$$

For the excitation of surface plasmon, the propagation constant of the excitation light should be equal to the propagation constant of the surface plasmon wave. Since the dielectric constant of metal is negative in sign, the propagation constant of surface plasmon wave is greater than that of direct light. This implies that the direct light cannot excite surface plasmons at a metal–dielectric interface and is referred to as non-radiative surface plasmons. Therefore, to excite surface plasmons, the momentum and hence the wave vector of the excitation light in dielectric medium should be increased. In other words, an extra momentum (and energy) must be imparted to light wave in order to get the surface plasmons excited at a metal–dielectric interface. This extra momentum is provided by the Kretschmann configuration. In Kretschmann configuration, a thin layer of metal is deposited on the base of a high refractive index prism. The dielectric medium of lower dielectric constant is kept in contact of the other surface of the metallic layer. When p-

S. K. Mishra · B. D. Gupta (✉)
Department of Physics, Indian Institute of Technology Delhi,
New Delhi 110016, India
e-mail: bdgupta@physics.iitd.ernet.in

polarized light is incident on the prism–metal interface through one of the faces of the prism the evanescent wave propagating along the interface excites the surface plasmon wave. If the intensity of the reflected light is measured as a function of incident angle, a sharp dip is observed at the resonance angle. Knowing this angle, one can determine the dielectric constant of the dielectric medium.

The prism-based SPR sensor has a number of shortcomings such as its bulky size and the presence of various optical and mechanical moving parts. Further, it cannot be used for remote sensing. These can be removed if an optical fiber, in place of prism, is used. In the case of optical fiber, the cladding is removed from a small portion of the fiber and the unclad core is coated with the metal. The dielectric medium is kept in contact of the metal layer. The advantages of optical fiber are miniaturized probe and remote and online sensing in addition to simplified optical design. Due to these advantages, fiber-optic SPR sensors have drawn lot of attention [3–10]. In fiber-optic SPR sensors, generally, wavelength interrogation method is used. Typically, gold or silver is coated on the core of the optical fiber to excite surface plasmons. Both of these metals have certain advantages and disadvantages. Silver is chemically more active than gold and gets oxidized quickly whereas gold is chemically stable and show higher shift in the resonance wavelength with small change in the refractive index of the dielectric or sensing medium. The thin layers of both of them are not continuous but agglomerate as islands [11]. In addition, band-to-band transitions (transitions which do not involve the conduction electron) take place in the visible range for gold layers [11]. The roughness on the surface of the metal film may also occur due to the thermal evaporation condition.

Recently, thin film-based sensors for toxic gases have attracted much attention due to the growing concern of environmental safety. Most of the conducting metal oxides (CMOs) have been found very suitable for gas sensing applications. Their properties have been found to be such that they can support the surface plasmon wave at the interface of the dielectric and CMO [12–14]. A number of metal oxides such as ZnO, SnO₂, and In₂O₃ have been used for the gas sensing applications [15–17]. Indium–tin oxide (ITO) shows the better result in comparison to gold and silver for surface plasmon. It is an n-type semiconductor that shows the high electrical conductivity and high optical transparency to visible light. There are no islands formation on even a very thin layer of it deposited on the dielectric surface. Further, no band-to-band transitions are involved in its case [12, 13]. The thin films of ITO are prepared by different techniques such as chemical vapor deposition [18], pulsed laser deposition [19], dc magnetron sputtering [20], and spray pyrolysis [21].

Hydrogen gas is used in a large number of applications but in the recent years its interest has increased due to its potential applications in the energy technologies. Hydrogen, due to its

smallest size, can migrate easily and hence can change the surface properties of the host material. It is a highly combustible gas with a lower explosive limit (LEL) of 4.65 % at room temperature and atmospheric pressure. Due to this, hydrogen gas leak detection has a security issue and therefore fast and reliable sensors for the detection of hydrogen gas are required [22]. A number of hydrogen sensors have been reported in the literature. Most of these are based on absorption of hydrogen gas by palladium resulting in the change in its optical properties. The ability to detect hydrogen gas leak economically and with inherent safety is an important issue that could facilitate commercial acceptance of hydrogen gas in various applications. It is therefore important that the sensor be very economical. Optical fiber-based sensors that are cheap have a number of advantages mentioned above and hence can be utilized for the detection of hydrogen gas.

In this paper, we report the fabrication and characterization of a fiber-optic sensor utilizing the surface plasmon resonance of ITO films for the detection of hydrogen gas in a nitrogen gas atmosphere. ITO is used because its film is better than silver or gold as mentioned above and is cheaper than these metals. For the fabrication of the fiber-optic probe, a small portion of the unclad core of the fiber is coated with a thin film of ITO. When hydrogen gas comes in contact of ITO, it changes the optical properties of the ITO film and hence the SPR spectrum recorded at the output end of the fiber when light is launched in the fiber from a polychromatic source. The composition ratio of ITO and the thickness of ITO film have been optimized for the best performance of the sensor. The advantage of ITO over palladium is that the performance of the sensor can be enhanced by choosing proper composition of ITO.

Experimental

Preparation of the Probe

For the fabrication of the SPR probe, 1 cm length of the cladding is removed from the middle portion of the plastic clad silica fiber of 600- μm core diameter and 0.4 numerical aperture from the total length of about 25 cm. The unclad portion of the fiber was first cleaned with acetone and then with methanol in the ultrasonic bath. It was further cleaned by high-tension ion plasma bombardment in a vacuum chamber at the chamber pressure of 5×10^{-4} mbars. After cleaning, the unclad portion of the fiber was coated with ITO layer of different composition and thicknesses using thermal evaporation technique in a vacuum coating unit kept at 5×10^{-6} mbars pressure.

Experimental Setup

A schematic of the experimental setup is shown in Fig. 1. After the fabrication of SPR probe, it is fixed in the gas

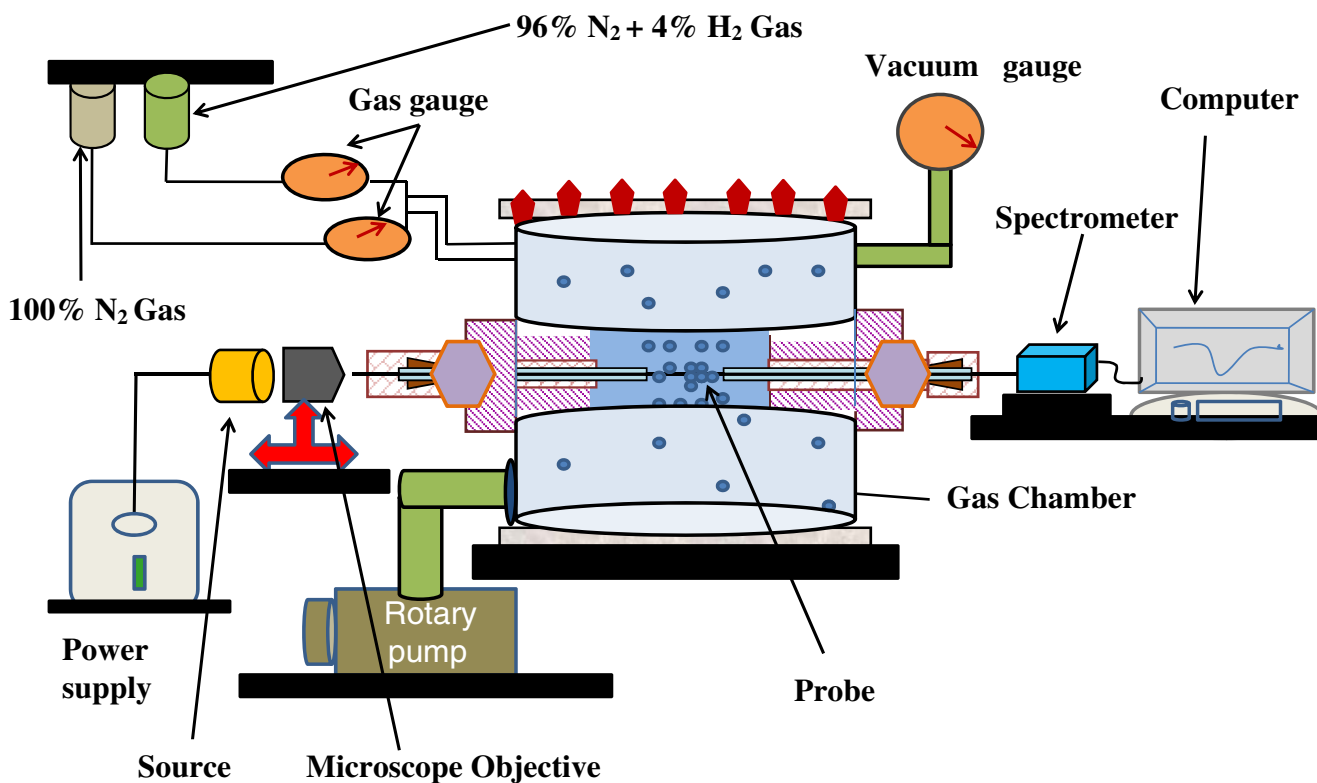


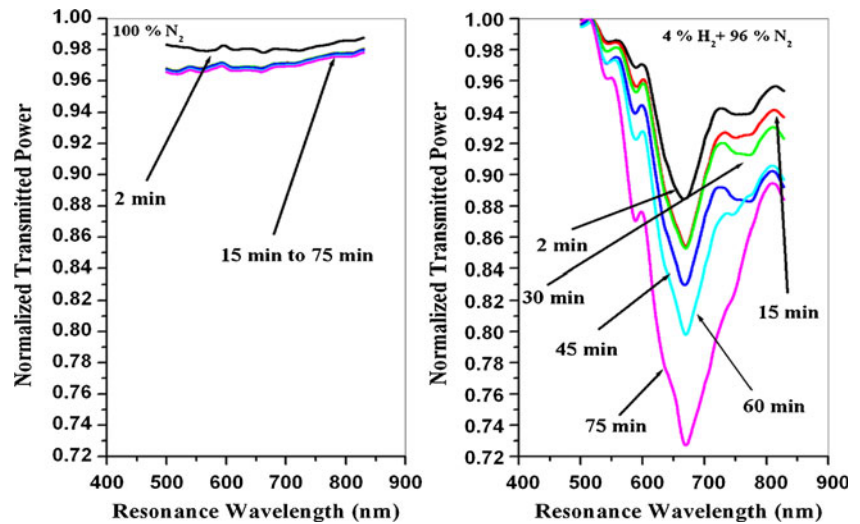
Fig. 1 Schematic diagram of the experimental setup of fiber-optic hydrogen gas sensor

sensing chamber, having facility of inlet and outlet for the gases. The evacuation of the chamber is carried out by rotary pump and the pressure of the chamber is monitored by the vacuum gauge. For our gas sensing studies, we have used two gas cylinders, one of which contains 100 % nitrogen while the other one contains 4 % hydrogen in 96 % nitrogen in volume ratio. These cylinders were connected to gas chamber using steel piping and can be used separately using shut-off valves. Unpolarized light from a tungsten-halogen lamp (AvaLight-HAL) was launched into the input end of the fiber with the help of a microscope objective. The spectrum of the transmitted power at the other end of the fiber was recorded with the help of a spectrometer (AvaSpec-3648) interfaced with a computer. To study the performance of the sensor, the chamber was first evacuated by rotary pump and the reference spectrum was recorded. All the spectra taken in the present study for different combination of gases were recorded with reference to this one. Gas from a cylinder having 100 % nitrogen was then connected to the gas chamber and the SPR spectra were recorded at fixed interval of time. To obtain SPR spectra for the mixture of 4 % hydrogen and 96 % nitrogen, the nitrogen was first evacuated from the gas chamber by the rotary pump and then the mixture of gases was introduced in the chamber. Again, the SPR spectra were recorded at fixed interval of time. In all the cases, while recording the SPR spectra, the pressure of the gas chamber was maintained at 1 atm.

Results and Discussion

In Fig. 2, we plot the SPR spectra for the nitrogen gas as well as the hydrogen–nitrogen mixture at different intervals of time, varying from 2 to 75 min for composition of the ITO ($\text{In}_2\text{O}_3:\text{SnO}_2$) as 70:30 and 90 nm thickness of the ITO layer. A dip in the SPR spectrum is observed around 669 nm in the case of mixture of hydrogen with nitrogen while no dip is observed in the case of nitrogen in the visible region. Further, a negligibly small shift in the resonance wavelength is observed with the introduction of mixture of hydrogen in nitrogen environment with time. However, the decrease in transmitted power occurs with the increase in time due to the reaction of hydrogen gas with the ITO layer. All these changes occur due to the formation of ITO hydride when hydrogen comes in contact of ITO resulting in the change in the electrical, optical, and chemical properties of ITO. From the SPR spectra shown in Fig. 2, it appears that the real part of the dielectric constant of the ITO layer changes slowly while the imaginary part changes fast resulting in no shift in resonance wavelength while continuous decrease in transmitted power occurs with time. In other words, the absorption of light at a particular wavelength (or resonance wavelength) increases with increasing time duration in gaseous environment. Further, nitrogen does not affect the dielectric constant of the ITO layer. The experiments have also been carried out for different compositions of ITO. Figure 3 shows the

Fig. 2 SPR spectra of fiber-optic probe for 100 % nitrogen and for a mixture of 4 % hydrogen and 96 % nitrogen at different times after filling the gas in the chamber. The composition of ITO ($\text{In}_2\text{O}_3:\text{SnO}_2$) is 70:30 and the thickness of the ITO layer is 90 nm



variation of resonance wavelength with the composition of the ITO ($\text{In}_2\text{O}_3:\text{SnO}_2$). For these measurements, the ITO film thickness was kept as 70 nm. In the figure, filled squares are the experimentally observed resonance wavelengths while the continuous line is the best fit. It may be observed that as the concentration of tin oxide in indium oxide increases, the resonance wavelength increases which indicate that the refractive index of the ITO thin film increases with the increase of tin oxide concentration in indium oxide. Thus by varying the composition of ITO, the resonance wavelength can be tuned which is one of the advantages of using ITO for the gas detection.

To see what composition will give maximum change in transmitted power after introducing the mixture of hydrogen and nitrogen gases in the chamber, we, in Fig. 4, have plotted the difference in normalized transmitted power between N₂ in chamber only and the mixture of 96 % N₂ and 4 % H₂ in chamber at the resonance wavelength with the composition of ITO after 2 min of introducing gas in the chamber. For all the composition, the thickness of the ITO layer was 70 nm. It may

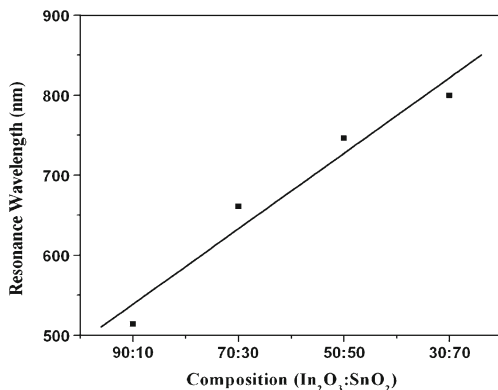


Fig. 3 Variation of resonance wavelength with the composition of ITO ($\text{In}_2\text{O}_3:\text{SnO}_2$) for ITO film thickness as 70 nm

be noted from the figure that the difference in the normalized transmitted power at resonance wavelength is maximum for 70:30 ($\text{In}_2\text{O}_3:\text{SnO}_2$) composition of ITO. In other words, 70:30 composition of ITO is the optimized composition for ITO to give maximum sensitivity for the hydrogen gas sensing. Similar kinds of results have also been reported for the sensors based on electrical properties of ITO.

To optimize the thickness of ITO layer, experiments have also been carried out for different thicknesses of ITO layer. In Fig. 5, variation of resonance wavelength with the thickness of ITO layer for optimized composition of ITO ($\text{In}_2\text{O}_3:\text{SnO}_2$), 70:30, has been plotted. The figure shows that with the increase in the ITO layer thickness the resonance wavelength increases. Again, the thickness of ITO layer can be used to tune resonance wavelength.

To see what thickness of ITO layer will give maximum change in the transmitted power after introducing hydrogen

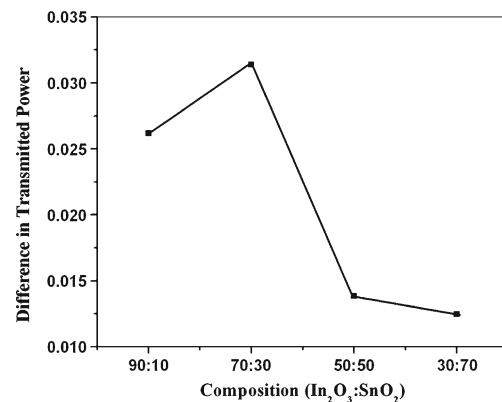


Fig. 4 Variation of difference in normalized transmitted power between N₂ in chamber only and the mixture of N₂ and H₂ in chamber at the resonance wavelength with the composition of ITO ($\text{In}_2\text{O}_3:\text{SnO}_2$) after 2 min of introducing gas in the chamber. For all the composition, the thickness of the ITO layer was 70 nm

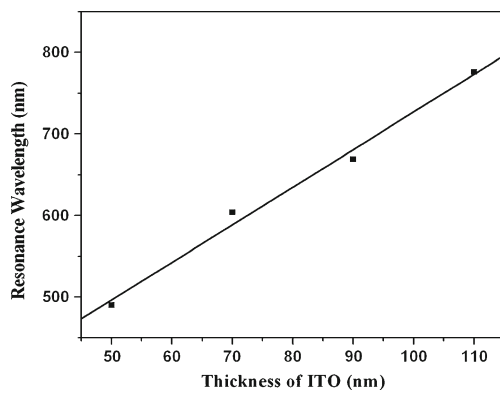


Fig. 5 Variation of resonance wavelength with the thickness of the ITO layer for the composition of ITO ($\text{In}_2\text{O}_3:\text{SnO}_2$) as 70:30

and nitrogen gas mixture in the chamber, we, in Fig. 6, have plotted the difference in normalized transmitted power between N_2 in chamber only and the mixture of 96 % N_2 and 4 % H_2 in chamber at the resonance wavelength with the thickness of ITO layer after 2 min of introducing gas in the chamber. For all the thicknesses of the ITO layer, the composition was 70:30. It may be noted from the figure that the difference in the normalized transmitted power at resonance wavelength is maximum for 90 nm thickness of ITO layer. In other words, 90 nm thickness of ITO layer is the optimized thickness for ITO to give maximum sensitivity for the hydrogen gas sensing. All these results indicate that 70:30 is the optimized composition of ITO and 90 nm is the optimized thickness of ITO layer for the maximum sensitivity of the sensor for the detection of hydrogen gas.

The dependence of the performance of various sensors utilizing different physical properties of ITO on its composition has also been reported earlier. It has been reported that with the increase of tin oxide concentration in indium oxide,

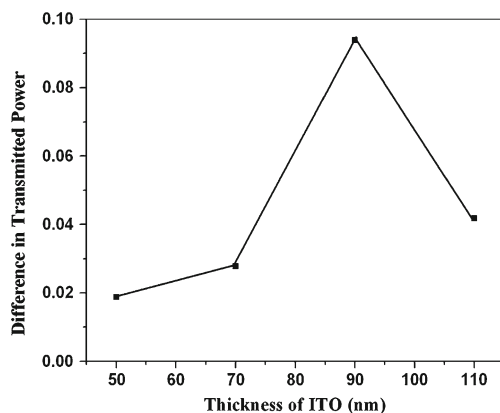


Fig. 6 Variation of difference in normalized transmitted power between N_2 in chamber only and the mixture of N_2 and H_2 in chamber at the resonance wavelength with the thickness of ITO layer after 2 min of introducing gas in the chamber. The composition of ITO ($\text{In}_2\text{O}_3:\text{SnO}_2$) was 70:30

the grain size of the ITO decreases and also changes the morphology of the ITO. As a consequence of grain size reduction, the surface available for the gas target–sensing layer interaction is maximized. In addition, the increase of tin oxide concentration in indium oxide concentration changes the electrical resistance (conductivity) of ITO. For sensing carbon monoxide gas (CO) and ethanol at high temperatures, the electrical properties of ITO have been used. These analytes change the electrical properties of ITO. The response of the sensor for the analytes depends on the composition of ITO. Initially, it decreases strongly on adding tin oxide attaining a minimum value and then increases on further adding tin oxide. The minimum value is obtained around 15 % of tin oxide. The maximum response is achieved around 90 % of tin oxide in indium oxide [23]. Indium–tin oxide (ITO) thin film has also been used for the detection of methanol at room temperature. The sensor shows a maximum sensitivity for 17 % tin oxide concentration in indium oxide for methanol vapor [24]. In the present study, the best performance for hydrogen sensing is achieved for 30 % tin oxide concentration. These studies suggest that there is no fixed composition of ITO to give best performance of the sensor for different analytes. Thus one should use only that composition which gives best performance and avoid the interference of any other analyte.

It may be noted that in the present study, three-medium configuration, namely a fiber core, metal oxide thin film, and gaseous environment, has been used. Out of these three, two are semi-infinite dielectric media. For such kind of multilayer system the resonance wavelengths are determined by using Fresnel's reflection equations [14]. The equality of propagation constants of surface plasmon wave and evanescent wave as the resonance condition and mentioned in introduction is applicable for two semi-infinite media (metal and dielectric).

Conclusion

Fabrication and characterization of ITO-coated surface plasmon resonance-based fiber-optic hydrogen gas sensor have been carried out. The sensor operates in intensity modulation scheme and utilizes the reactivity of hydrogen gas with ITO, giving rise to changes in the dielectric constant of ITO which results in the change in the transmitted power. The 70:30 ($\text{In}_2\text{O}_3:\text{SnO}_2$) composition and 90 nm thickness of the ITO layer show maximum sensitivity with hydrogen. However, the operational wavelength can be tuned by changing the composition or the thickness of the ITO film.

Acknowledgments The present work is partially supported by the Council of Scientific and Industrial Research (India).

References

1. Homola J, Yee SS, Gauglitz G (1999) Surface plasmon resonance sensor: review. *Sens Actuators B* 54:3–15
2. Sharma AK, Jha R, Gupta BD (2007) Fiber-optic sensors based on surface plasmon resonance: a comprehensive review. *IEEE Sens J* 7:1118–1129
3. Jorgenson RC, Yee SS (1993) A fiber optic chemical sensor based on surface plasmon resonance. *Sens Actuators B* 12:213–220
4. Homola J, Slavik R (1996) Fiber optic sensor based on surface plasmon resonance. *Electron Lett* 32:480–482
5. Cheng SF, Chau LK (2003) Colloidal gold-modified optical fiber for chemical and biochemical sensing. *Anal Chem* 75:16–21
6. Kim YC, Peng W, Banerji S, Booksh KS (2005) Tapered fiber optic surface plasmon resonance sensor for analyses of vapor and liquid phases. *Opt Lett* 30:2218–2220
7. Rajan, Chand S, Gupta BD (2006) Fabrication and characterization of a surface plasmon resonance based fiber optic sensor for bittering component- naringin. *Sens Actuators B* 115:344–348
8. Rajan, Chand S, Gupta BD (2007) Surface plasmon resonance based fiber optic sensor for the detection of pesticide. *Sens Actuators B* 123:661–666
9. Srivastava SK, Verma R, Gupta BD (2011) Surface plasmon resonance based fiber optic sensor for the detection of low water content in ethanol. *Sens Actuators B* 153:194–198
10. Bhatia P, Gupta BD (2011) Surface plasmon resonance based fiber optic refractive index sensor: sensitivity enhancement. *Appl Opt* 50:2032–2036
11. Rhodes C, Franzen S, Maria JP, Losego M, Leonard DN, Laughlin B, Duscher G, Weibel S (2006) Surface plasmon resonance in conducting metal oxides. *J Appl Phys* 100:054905
12. Rhodes C, Cerruti M, Efremenko A, Losego M, Aspens DE, Maria JP, Franzen S (2008) Dependence of plasmon polaritons on the thickness of ITO thin films. *J Appl Phys* 103:093108
13. Franzen S, Rhodes C, Cerruti M, Gerber RW, Losego M, Maria JP, Aspens DE (2009) Plasmonic phenomenon in indium tin oxide and ITO-Au hybrid films. *Opt Lett* 34:2867–2869
14. Verma RK, Gupta BD (2010) Surface plasmon resonance based fiber optic sensor for the IR region using a conducting metal oxide film. *J Opt Soc Am A* 27:846–851
15. Gupta SK, Joshi A, Kaur M (2010) Development of gas sensors using ZnO nanostructures. *J Chem Sci* 122:57–62
16. Patil GE, Kajale DD, Chavan DN, Pawar NK, Ahire PT, Shinde SD, Gaikwad VB, Jain GH (2011) Synthesis, characterization and gas sensing performance of SnO₂ thin films prepared by spray pyrolysis. *Bull Mater Sci* 34:1–9
17. Suche M, Katsarakis N, Christoulakis S, Nikolopoulou S, Kiriakidi G (2006) Low temperature indium oxide gas sensors. *Sens Actuators B* 118:135–141
18. Maruyama T, Fukui K (1991) Indium tin oxide thin films prepared by chemical vapour deposition. *Thin Solid Films* 203:297–302
19. Zheng JP, Kwok HS (1993) Low resistivity indium tin oxide films by pulsed laser deposition. *Appl Phys Lett* 63:1–3
20. Ali MKM, Ibrahim K, Hamad OS, Eisa MH, Faraj MG, Azhari F (2011) Deposited indium tin oxide (ITO) thin films by dc-magnetron sputtering on polyethylene terephthalate substrate (PET). *Rom J Phys* 56:730–741
21. Korotcenkov G, Brinzari V, Schwank J, DiBattista M, Vasiliev (2001) Peculiarities of SnO₂ thin film deposition by spray pyrolysis for gas sensor application. *Sens Actuators B* 77:244–252
22. Bevenot X, Trouillet A, Veillas C, Gagnaire H, Clement M (2000) Hydrogen leak detection using an optical fiber sensor for aerospace applications. *Sens Actuators B* 67:57–67
23. Neri G, Bonavita A, Micali G, Rizzo G, Pinna N, Niederberger M, Ba J (2008) Effect of the chemical composition on the sensing properties of In₂O₃-SnO₂ nanoparticles synthesized by a non-aqueous method. *Sens Actuators B* 130:222–230
24. Patel NG, Patel PD, Vaishnav VS (2003) Indium tin oxide (ITO) thin film gas sensor for detection of methanol at room temperature. *Sens Actuators B* 96:180–189